A case study on internal flow patterns of the two-phase closed thermosyphon (TPCT)

S. Sichamnan [a], T. Chompookham [a], T. Parametthanuwat [b,*]

[a] Heat Pipe and Thermal Tool Design Research Unit (HTDR), Division of Mechanical Engineering, Faculty of Engineering, Mahasarakham University, Thailand
[b] Heat Pipe and Nanofluid Technology Research Unit, Faculty of Industrial Technology and Management, King Mongkut's University of Technology North Bangkok, Thailand

A B S T R A C T

This study investigates types of two-phase flow patterns that affect the heat transfer rate which occurs within the two - phase closed thermosyphon (TPCT) made of heat-resistant glass tube with inner diameters of 7 and 25.2 mm. Aspect ratio was 5 while the inclination angels were 0°, 80° and 90°, and the evaporator temperature were 50, 70 and 90 °C. Furthermore, the addition rate of chemical reactants was 50% by volume of the evaporator component whilst the water temperature within the condensation unit was maintained at 20 °C. From the experimental results, the TPCT's inner diameter was 7 mm, the inclination angels were at 80° and 90°. There were four types of flow pattern including; bubble flow pattern, slug flow pattern, churn flow pattern and annular flow pattern. Churn flow pattern and the annular flow pattern affected the heat transfer rate of the TPCT with the inner diameter of 7 mm at the inclination angels of 80 and 90° respectively. As for the TPCT test, the inner diameter of 25.2 mm with the inclination angels of 80° resulted in four types of the flow patterns, including the bubble flow pattern, slug flow pattern, churn flow pattern and stratified flow pattern respectively. According to the results, churn and stratified flow patterns, were the types of flow that affected the heat transfer rate. According to the experiment of TPCT with inner diameter of 25.2 mm at the inclination angels of 90°, four flow patterns including the bubble pattern, slug flow pattern, churn flow pattern and the vortex flow pattern were found. The vertex flow pattern was initiated when the temperature of the evaporator section was raised from 70 to 90 °C. According to this experiment, the churn flow and the vortex flow patterns were able to affect the heat transfer rates. Furthermore, the experiment revealed that heat flux that was obtained from the experiments of TPCT with the inner diameter of 7 and 25.2 mm showed the highest heat transfer rate at evaporation temperature of 90 °C and the inclination angels of 80° which were 31.88 and 58.15 W, respectively.

1. Introduction

The two-phase closed thermosyphon (TPCT) is a type of heat exchanger known to have the high efficient heat transfer rate even at the slightest different temperature between the heat source and the heat sink. The TPCT exhibits three main components, the evaporator section, adiabatic section and condenser section which have been made from copper pipes, stainless steel tubes, and carbon steel

---

pipes. Both ends of the pipe are closed while the interior is presented as a vacuum that contains the working fluids as shown in Fig. 1 (a). TPCT works when the heat receptor of the evaporator receives the heat from the heat source through the pipe's surfaces [1–3]. As the surface temperature of the pipe is gradually raised until surpassed the saturated temperature of the working fluids which resulted in the transference of heat from the pipe's surface to the working fluids [4]. As a result, viscosity and density of the working fluids have been decreased. When the temperature of the evaporator increases, differences between the temperature of the pipe's surface and that of the working fluids also increased which resulting in a condensation of vapor, and a flow of fluid. Consequently, a bubble flow with accumulated energy in the form of velocity and pressure where the increasing speed resulting in a collision between a vapor bubble [5]. Thus, the vapor bubble is merged and becomes larger similar to a bearing which is also known as a slug flow. Thereafter, when the vapor bubble came into collision with the head of the slug flow, a change in the flow pattern will occur for which the slug flow pattern is turned into churn flow [6]. At a higher speed, the bubble will cause a void in the middle of the pipe where the gas flows whereas the working fluid liquid is coated on the surface of the pipe. This flow patterns is also known as annular flow as shown in Fig. 1 (b). The flow will move up to the condenser section where the heat will be lost and the condensed liquid will subsequently reflow back into the evaporator section due to the gravitational force. The returned liquid will be reheated once again. This nature of the cycle will occur repeatedly. In terms of application, TPCT is suitable for both industrial processes and heat dissipation equipment for various engineering systems, including electronic systems cooling such as laptop computers, solar power systems and, air warming system [7]. The annular and churn flow patterns are capable of affecting the heat transfer rate [8–10]. Therefore, efforts have been made to improve properties of the original working fluid in order to boil it faster which leads to changes the flow patterns rapidly by maintaining the condition of the annular and churn flow patterns at a relatively high percentage of occurrence [11]. Therefore, to heighten the properties of the original working fluids that were relatively low has become the objective of this research. The researched focused on studying of two-phase flow patterns that affect the heat transfer rate where silver nanoparticles and adding oleic acid have been added to reduce surface tension in the original working fluids that applied to the TPCT.

The heat transfer characteristics within the TPCT are subjected to the basis of the internal flow pattern depending on different heat transfer capacity, such as inner diameter, length of the tube, inclination angel, filling ration, evaporator temperature, and type of working fluid. The flow pattern and internal flow behavior of TPCT has been a subject of studies and presentation by many researchers, such as the study of TPCT's internal flow patterns with inner diameter of 11.1 mm, inclination angles of 90°, 30°, and 5° against the horizontal axis. In this research, R123 was used as the working fluid while the vapor temperature was 30 °C, the aspect ratios was 30, 10, and 5, and the addition ratio was 80% [8]. The results revealed that the aspect ratio was 30 and an inclination angle was 90°, and the maximum heat flux was 20.7 kW/m². At the top of the evaporator section, annular flow (AF) was discovered, while the churn flow (CF) and slug flow (SF) were found in the middle part of the evaporator section. The lower part of the evaporator section was where the bubble flow presented, the main flow pattern found in inclination angles of 90° was the annular flow and churn flow that were combined with the slug flow. At the inclination angles of 30° and the maximum heat flux of 24.6 kW/m², bubble flow (BF) was found and appeared throughout the lower part of the evaporator section. In the middle part of the evaporator section, the slug flow with
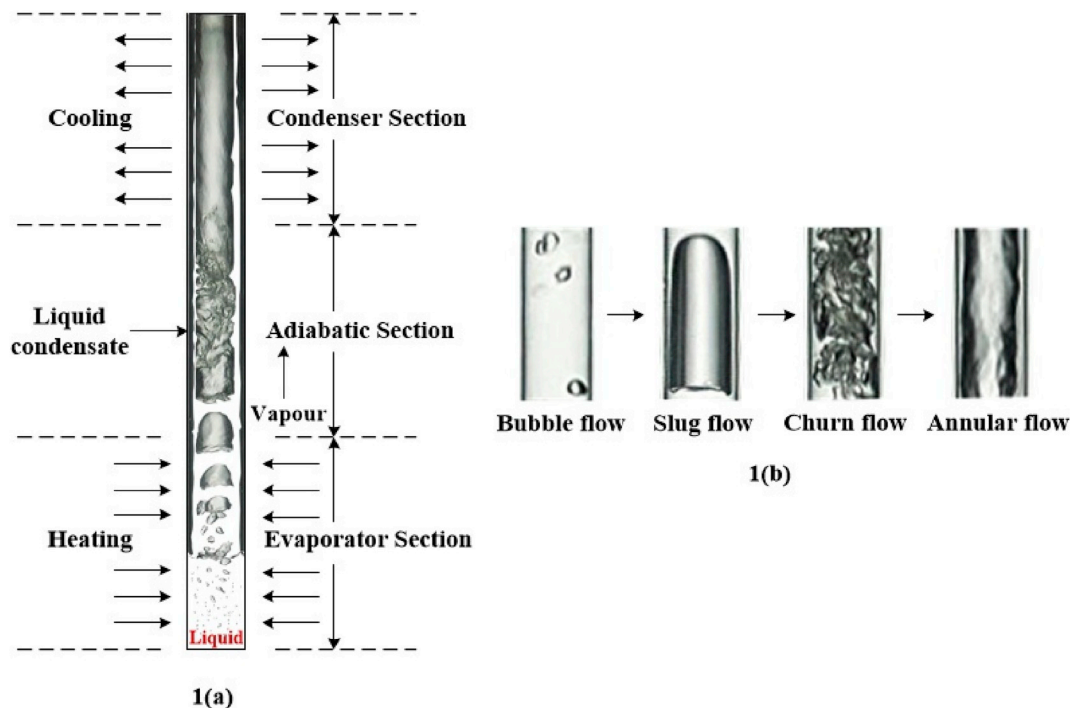

Fig. 1. (a) Two phase closed thermosyphon (TPCT) and 1(b) Two – Phase Flow Pattern.

high-expansion liquid waves located adjacent to each other was found. While the stratified flow occurred at the top of the evaporator section, bubble flow and slug flow were the main flow patterns found at the inclination angles of 30°. At the inclination angles of 5°, the maximum heat flux was 16.7 kW/m^2, and the slug flow was found in combination with the wave liquid at the lower and middle parts of the evaporator section. At the top of the evaporator section, the slug flow was formed as a result of the liquid splash from the lower part. The main flow pattern found in the inclination angles of 5° was the bubble and slugs with a slightly expanded fluid waves. The results also revealed that the aspect ratios of 10, almost all of the internal flow patterns were quite similar to that of aspect ratios 30 [10,11]. As per the ratios 5 of inclination angles 90°, 30° and 5°, the maximum heat flux of each inclination angles was 78.6, 92.4 and 53.9 kW/m^2, respectively. Bubble flow and the main flow was in the inclination angle of 5° [8]. From the study of the flow patterns and the use of different working fluid such as ethanol and HFE-700, experiments with the TPCT, inner diameter 8 mm, length of evaporator section 100 mm, length of adiabatic section 180 mm and length of condenser section 200 mm. For the use of water and ethanol as working fluid, tested with heat flux were conducted at 7.5 and 7.0 kW/m^2 respectively. Geyser boiling occurs, low vapor pressure and high bubble production rate and found slug flow and plug flow at the test with heat flux were 5.5 and 5.5 kW/m^2 respectively, high vapor pressure, and low bubble production rate. Churn flow was found when tested with heat flux at 17 kW/m^2, which occurred at the high vapor pressure, high rate of bubble production and the surface tension was relatively low when ethanol was used as working fluids. When using HFE-700 as a working fluid, the experiment revealed the heat flux of 7.8–21.5 kW/m^2 the characteristics of the pool boiling. At the evaporator section, the high bubble production rate and the size of the bubble were less than those of water as working fluid [9,13]. The phenomenons of liquid condensation that reflow into the evaporation were less when using HFE-700 as working fluid. This was due to the low surface tension properties when compared to ethanol [9]. From the experiment of the TPCT, graphene-acetone nanofluids at the concentrations of 0.05%, 0.07% and 0.09% were used as working fluid. The heating values of the evaporator were between 10 and 50 W. Upon heating the evaporator at 10 W, the bubble flow discontinued and the average size was less than the diameter of the pipe. When increased the heat by 20 W to the evaporator, the bubble flow pattern and the number of bubbles were increased. Upon increasing the heat to the evaporator by 30 W, churn flow was observed within the TPCT. When the evaporation heat was increased to 40 and 50 W, the flow pattern changed from churn flow to annular flow. In addition, the heat resistance was reduced to 70.3% and the heat transfer coefficient of the evaporator was increased to 61.25%. When using Graphene-acetone nanofluids at the concentrations of 0.09%, the annular flow, compared to other flow patterns, provided higher heat transfer coefficients [10]. Observation of the internal flow pattern of the two- TPCT made of glass tubes when using ethanol as a working fluid, showed that the behavior and flow patterns that occurs within TPCT. Upon considering the TPCT work cycle, this begins with the evaporation of the heated TPCT, and the working fluid in the liquid phase starts to boil and transformed from liquid to vapor, flows pass the adiabatic section to the condenser section and condenses at the top of the TPCT. The surface between vapor and liquid in the middle of the TPCT, at the same time the evaporation of vapors from the evaporator section, becomes vaporized below the condensation [10,14,15]. The cough is blocked by the condensed vapor in the condenser section and some drop to the evaporator section. At the same time, the vapor is created in the evaporator section and the condensed liquid flows into the lower part [6]. The flow pattern within the device can also be used as an indicator of system stability. The study of characteristics flow instabilities in a horizontal thermosyphon reboiler loop was conducted and the experiment was carried out using liquid water in the process and the steam was the medium for heat transfer. The liquid flow rate was the major factor of the instability because it was of variable height widths and vibrations. A stabilized system has a heat flux of greater than 20 kW/m^2. The usual system has heat flux between 11 and 20 kW/m^2. The flow pattern that occurred in the system influenced the liquid flow rate because different flow patterns have different speeds and properties. The flow patterns detected during the test were mostly classified as basic flow patterns. Found annular pattern and have high heat flux and high quality flow. The heat flux decreases from the churn flow, slug flow and bubble flow respectively [16]. According to the study of flow patterns and heat transfer characteristics with the inner diameter of 4.26 and 2.01 mm, 6 flow patterns namely; dispersed bubble flow, bubbly flow, slug flow, churn flow, annular flow and mist flow were discovered. Changing the inner diameter from 4.26 to 2.01 mm resulted in a change in flow pattern from slug flow to churn and annular flows. Convection caused by two-phase flow patterns in the pipe, where the heat transfer coefficient was a function of the heat flux and system pressure. This was not subjected to the quality of the vapor and the mass of the flux. Results of the experiment with the inner diameter of 4.26 mm showed that the vapor quality was less than 40–50%. The heat transfer coefficient would increase in accordance with the flow rate of the heat and pressure of the system. As the quality of vapor was not altered in this period, the vapor featured was the nucleate boiling. For pipes with an inner diameter of 2.01 mm, the quality of the vapor was less than 20–30% [17]. The study of flow patterns of ethanol and a silver nano-ethanol mixture as working fluid in of a closed-loop oscillating heat-pipe with check valves using pyrex glass tube with inner diameter of 2.4 mm showed that the maximum flux of silver nano-ethanol mixture was 2.04 kW/m^2, while the evaporator temperature was 125 °C, and the inclination angels was 90°. The maximum heat flux when using ethanol as working fluid at 1.31 kW/m^2, and the evaporator temperature was 125 °C, with the inclination angels was 90°. The main flow patterns found in both cases were dispersed bubble flow with small bubbles appearing in the lower part of the evaporator section for which the bubbles were dispersed to the lower part of the evaporator section before moving to the condenser section [18].

The working fluid was another important variable affecting the behavior of internal flow patterns. This results in the heat transfer characteristics of TPCT and the heat pipe (HP). There have been attempts to improve the properties of the heat transfer of relatively low traditional working fluid such as water, ethanol, and others. Therefore, the nanofluids containing nanoparticles such as gold, brass, copper and silver have been developed which have been added to a traditional working fluid. Based on previous research, the use of nanoparticle fluid as working fluid with TPCT [19]. Silver-nanofluids, small particles affect the contact areas, generate more heat at higher proportion of heat dissipation than the base fluids or even traditional working fluid, thus, leads to quick and easy boiling of the working fluid [20]. In addition, the silver nanoparticle fluid also improved the heat transfer rate due to the high thermal conductivity (k), and resulted in a large proportion of vapor which was beneficial for the increase of the heat transfer rate [4]. Based on the available

examination data, the aspect ratios was 20 (inner diameter 25.4 mm) and the operating temperature was 60 °C, the heat transfer rate was 750.81 W, which was 70% higher compared to DI-water [10]. This demonstrated the increased thermal efficiency and improved convective heat transfer coefficient compared to the traditional working fluid [13,21,22]. In addition, the silver-nanofluids were found to reduce heat resistance in the heat pipe (HP) by 10–80%, compared to using DI-water as the heating agent for 30–60 W. The results showed that HP of thermal resistance decreased as the size of the nanoparticles and the concentration increased [23]. If heat resistance inside the pipe is lower, direct heat from the heat source to the evaporator section and the heat transfer from the wall to the working fluid became streamlined and fast. Apart from the boiling effect of the active ingredients, this could also lead to a better flow pattern change, respectively. TPCT efficiency increased to 14.7% when using Al_2O_3–nanofluids as working fluid for DI-Water. This was confirmed by the effect of temperature distribution on the surface of the TPCT [24]. To improve the heat transfer properties of heat pipes (HP), SiC-nanofluids have been used. As a result, the heat resistance of HP were decreased by 11%, 21% 30%, when using silicon carbide (SiC) at concentrations of 0.35, 0.70 and 1.0 wt% respectively. The maximum heat transfer of HP increased by 29% at a concentration of 1.0 wt% nanoparticles [25]. The performance of the TPCT increased with the use of ZrO_2-nanofluids as working fluid instead of DI-Water. The examination was conducted with TPCT made of copper tube which has an outside diameter of 6 and 8 mm, and 800 mm length while the concentrations of nanoparticles were 3 and 4 wt% [26]. The appearance of nanoparticles is coated or laminated in the heating part. According to the application of nano-fluid in TPCT at vertical position, water, titanium nano-water mixture, and gold nano-water mixture were used as working fluids. Then, examinations at different concentrations were applied. At maximum concentration between 0.2 and 0.3 vol%, the heat resistance value started to increase or rise again. As the nanoparticles were coated on the evaporator section surface, long-term test at a concentration of 0.3% showed a porous layer formed by the formation of nanoparticles on the evaporator section surface [27]. A study to explain the understanding of boiling flow with CuO-nanofluids as working fluid within the two-phase closed loop thermosiphon was conducted under constant atmospheric pressure. The results showed that the critical thermal flux increased as a result of the coated layer of nanoparticles on the surface of the heating element. This was due to the coating of nanoparticles and their properties [28]. A thin porous layer was formed at the structure of the wick which generated by the floating of nanoparticles in the nanofluids. This has showed that the increased thermal efficiency of the heat pipe was due to the porous layer of evaporator section. As the floor can expand the surface in the evaporator section, with higher heat transfer efficiency, can improve surface adhesion and adsorption efficiency [29,30].

Nanofluids are working fluid within the TPCT and heat pipes (HP) which could cause problems regarding condensation and the deposition of the nanoparticles in the base fluid. The stability and distribution of nanoparticles are not uniform when used on long term basis [31–33]. The precipitated nanoparticles caused the reductions of surface areas of the receiving and exhaling of the evaporator section and condenser section. When the evaporating area is reduced, the boiling of the working fluid will be directly affected which resulted in lower heat transfer efficiency. In addition, the deposition of nanoparticles led to impediment of fluid flow within the pipe, hence, became another cause of pipe erosion [34]. Efforts have been made to improve the stability and distribution of nanoparticles by means of mechanical stirring, ultrasonic treatment, and even modification of the surface of nanoparticle fluid by chemical means, such as adding of surfactant [35]. Another way to change the stability of nanoparticles is through surface conditions by showing the distribution of nanoparticles in the base fluid. As a result, the particle size and the density of the particles were less in the absence of surfactant. This resulted in better distribution behavior in the base fluid and higher thermal conductivity and the efficiency of distributed behavior as well as thermal conductivity. The surfactant addition method was a better choice than other surfactants addition [36]. The stability of nanoparticles was also related to the viscosity of nanoparticles as the good stability of the nanoparticle fluid decreased the viscosity and increased the thermal conductivity [37]. Various surfactants such as lauric acid (LA; C12), myristic acid (MA; C14), dodecyl-benzenesulphonic acid (DBSA, C16) and oleic acid (OA; C18) have been used to coat magnetite particles in order to dissipate the transformer oil (TR30) and Fe-nanoparticle fluid. Longer tensides chains reduce surface tension and viscosity better than the shorter ones by optimizing the length of the chain of the organic oleic acid (C18), which had a relatively high dispersion of particles and a stability of about 30%. Because of this, surfactants was capable of the surface tension of the working fluid and to increase the uniformity of the nanoparticles [38]. In addition, it was found that the distribution of Al2O3 nanoparticles, when surfactant Methacrylic acid (PMAA-NH4) and poly (acrylic acid) (PAA) were added. Poly (acrylic acid) (PAA), it is easier to distribute and absorb Al2O3-nanoparticles than the methacrylic acid (PMAA-NH4) which distributed relatively efficiency. Higher stress and viscosity were observed in PMAA-NH4 suspensions compared with PAA suspensions. Furthermore, flow behavior was better distributed and dispersed with 47.5% PAA suspension [39].

This study investigates types of two-phase flow patterns that affect the heat transfer rate which occurs within the thermosiphon and the application of silver nanoparticles with oleic acid to reduce surface tension of the working fluids. Based on the studied data about the two - phase flow patterns within TPCT information regarding silver nanoparticles and added oleic acid to reduce surface tension as working fluids within TPCT remains limited. This was to ascertain the advantages and disadvantages of nanoparticle powder application including methods or techniques for improving. Silver nanoparticle powder has a high thermal conductivity and a small nano scale which can increase the contact surface areas. Thus, more heat can be received. Furthermore, the addition of oleic acid as a surfactant also helps to disperse nano-silver powder in the working fluids, thus, regularly helps the working fluids to increase the efficiency of heat transfer. With qualitative data from the behavior of the flow pattern, knowing different types of flow patterns, the evaporator temperature, the inner diameter of thermosyphon, and the inclination angel can affect the heat transfer rate caused by the use of silver nanoparticles with oleic acid. The added components were intended to reduce surface tension as working fluids as obtained from this study. The information could also be used to describe the heat transfer rate that occurs which consequently lead to the design of TPCT that requires working fluids consisted of silver nanoparticles and added oleic acid. This would help to reduce surface tension for a higher work efficiency in the future.

2. The experimental apparatus and analysis

2.1. Method

Nano Silver Powder and oleic acid as prepared by a Sigma-Aldrich Inc, Milwaukee, Wisconsin: USA were used in this study. Silver nanoparticles were <100 nm, 99.9% metal basis. According to the preparation that involved two-step methods, physical technique of sonication in ultrasonic bath and stirrer were used respectively. The first step involving silver nanoparticles dispersion with 0.5 wt% concentration of the base fluids, the DI-Water, when the first step was accomplished, the silver nanoparticles were dispersed in the base fluids (NP). Thereafter, the second step was to ads the oleic acid (Surfactant) at 1 wt% of NP. This two-step method reduced the aggregation of nanoparticles and helped to achieve a homogeneous suspension shown in Table 1 [33,40].

2.2. The schematic diagram of the equipment, instrument setup and the two phase closed thermosyphon (TPCT)

Fig. 2 shows schematic diagram of the equipment and instrument setup. The controlled and variable parameters shown in Table 2. The vacuum is located inside the TPCT filled working fluids using the filling set as shown in Fig. 2a. The TPCT test set is shown in Fig. 3. TPCT received hot water from the hot bath before being passed to the evaporator section while the cold water from the cold bath was passed to the condenser section. The parameters in this study consisted of the TPCT made of Pyrex tube with an inner diameter of 7 and 25.4 mm, the working fluids were de-ionized water mixed with silver nanoparticles at the concentration of 0.5 wt% (NP) respect to total volume of water containing 1 wt% of Oleic acid (OA) respect to total volume NP and the filling ratio was 50% with respect to evaporator section respectively. The evaporator section temperatures were set at 50, 70, and 90 °C, while the aspect ratio was 5 and the inclination angle were at 0, 80, and 90° from the horizontal pane. The condenser section temperature was 20 °C and the mass flow rate of feed water was 0.25 L/min as show in Fig. 2b.

According to the experiments as show in Fig. 2b, the evaporator section of TPCT was soaked in the hot water within the glass box while the heat from the heater is regulated by temperature control. The condenser section of TPCT is cooled by cold water and the control flow rate of cold water with flow meter. Temperature data were measured by 9 points type k-thermocouples with ± 1.5 °C accuracy and Record by Data logger (Yokogawa DX200) with ±1°C accuracy. The flow meter used was Disco-BBBW1B98 with ± 5% accuracy. Temperature measurement consisted of, 1 point in hot water at the evaporator section, 2 points in the hot bath whereby 1 point was connected with the temperature control and 1 point was connected with the Data logger, 2 points at the adiabatic section, 1 point for environment, 1 point at inlet water of the condenser section, 1 point at outlet water of the condenser section and 1 point at the cold bath. Measurement of the outlet and inlet water temperature of the condenser section was used to determine the heat transfer rate that can be obtained from equation (1).

2.3. Heat transfer rate and flow patterns analysis

The heat transfer characteristics of the TPCT is initiated when the working fluids is contained within evaporator section of TPCT, which in a saturated phase, is heated by a heating source. Change of phase becomes vapor which flow pass the adiabatic section to the condenser section and where the surface area's temperature is lower than the evaporator section and leads to condensation from the heat transfer at the condenser section. Equation (1) can be used to determine the heat transfer rate in the condenser section by measuring the inlet and outlet water temperatures in the condenser section [41,42]:

$$Q = \dot{m} \, C_p (T_{co} - T_{ci}) \tag{1}$$

When Q is the heat transfer rate (W), $\dot{m}$ is the mass flow rate of the water (kg/s), C_p is the specific heat of the water (J/kg.°C), T_{co} is the outlet water temperature (°C) and T_{ci} is the inlet water temperature (°C).

And the mass flow rate of the water can be determined by

$$\dot{m} = \rho v A \tag{2}$$

Table 1
The methods of preparing silver nanofluids with oleic acid surfactant.

| Method of preparing nanofluids	Condition
Two-step method of silver nanofluids	The temperature was controlled at lower 25 °C.
Ultrasonic bath	Sonication time: 6 h. Frequency: 43 kHz.
Stirrer	Revolution time: 30 min
	Sonication time: 30 min
Ultrasonic bath	Frequency: 43 kHz.
Add oleic acid surfactant	The temperature was controlled at lower 25 °C.
Ultrasonic bath	Sonication time: 12 h.
	Frequency: 43 kHz.
	Revolution speed: 1000
Stirrer	Revolution time: 30 min
	Sonication time: 30 min
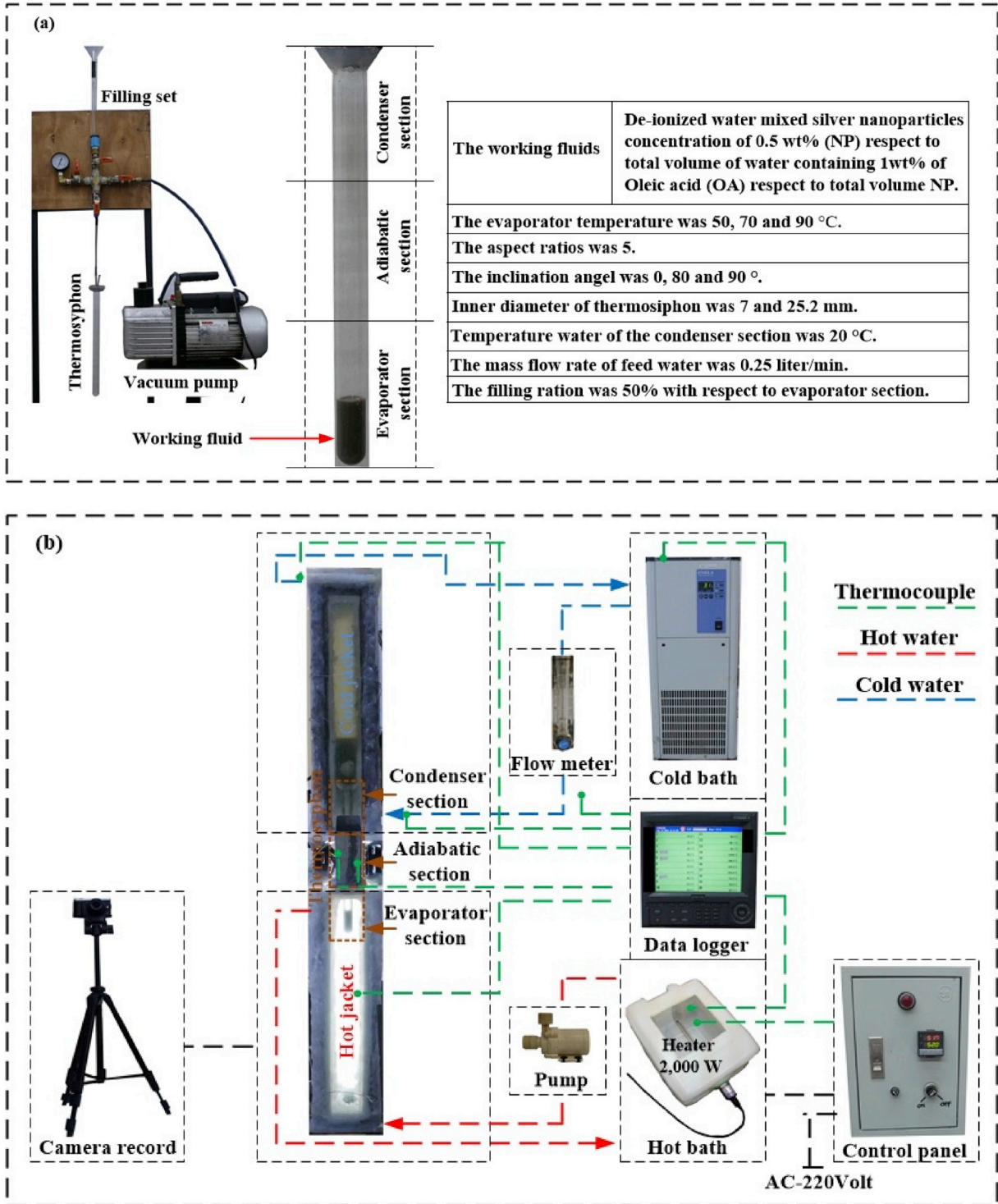
Fig. 2. The schematic diagram of the equipment and instrument setup.

When ρ is the water density (kg/m^3), ν is the water velocity (m/s), A is the cross-section area of water flow (m^2).
And the heat flux can be determined by Refs. [32,39].

$$q = \frac{Q}{A_c} = \frac{Q}{\pi D_o L_c N}$$
(3)

Table 2
Controlled and variable parameters.

| Conditions	
Independent variables	• The evaporator temperature at 50, 70 and 90 °C. • The inclination angel of 0, 80 and 90°. • The inner diameter of thermosyphon of 7 and 25.2 mm.
Control variables	• The working fluids; De-ionized water mixed with silver nanoparticles at the concentration of 0.5 wt% (NP) respect to total volume of water containing 1 wt% of oleic acid (OA) respect to total volume NP. • The aspect ratios was 5. • The temperature water of the condenser section was 20 °C. • The mass flow rate of feed water was 0.25 L/min. • The filling ratio was 50% with respect to evaporator section.
Dependent and variables	• The effect of the evaporator temperature, the inner diameter of thermosyphon the inclination angel to the flow patterns two-phase closed thermosyphon. • The effect of the evaporator temperature, the inner diameter of thermosyphon and the inclination angel to heat transfer rate and heat flux two-phase closed thermosyphon (TPCT).
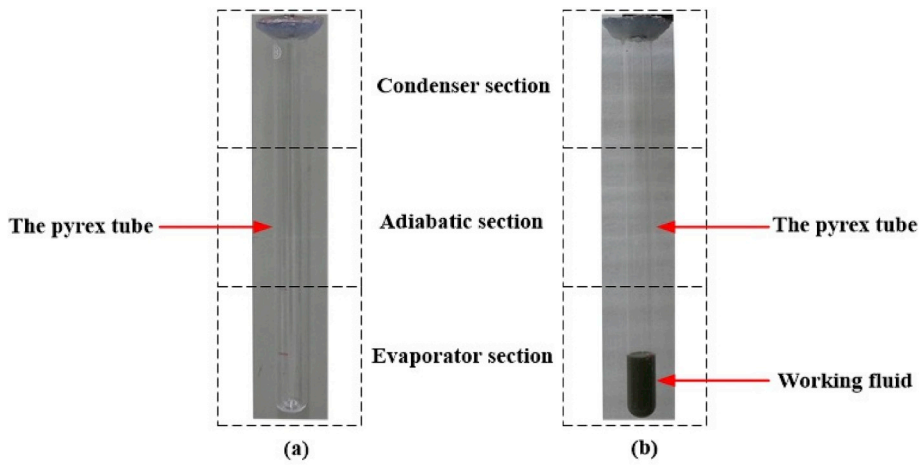
Fig. 3. The TPCT used in this study.
(a) Before filling the working fluid (b) After filling the working fluid.

When q is the heat flux (W/m^2), Q is the heat transfer rate (W), D_o is the outside diameter of the tube (m), A_c is the total external area of the tube (m^2), L_c is the condenser section length (m), N is the number of TPCT in the condenser section.

The visualized flow patterns of the TPCT were recorded by a continuous video camera that produced slides at 60 frames rate. The percentage of each flow pattern was determined by area (length x wide) of vapor in each flow pattern. The percentage of flow pattern was an average value of working fluids flow which occurs 3 cycles of recorded video for each condition.

The percentage of each flow pattern can be determined by

$$(\%) \text{ each flow pattern} = \frac{\text{Number of grid found for each flow pattern}}{\text{Total Grid}} \times 100 \tag{4}$$

When the number of Grids is the number of assumptions used for the period at position or space to work with images flow patterns. It is a table with the same spacing of each channel.

2.4. Uncertainty analysis

Measurement of uncertainty, the calculations are divided into 2 types. Type A is the uncertainty due to a random source that has been evaluated statistically which can be calculated from the following equation.

By $\bar{x}$ is arithmetic mean and SD is standard deviation

$$\bar{x} = \frac{x_1 + x_2 + \dots + x_n}{n_s} \tag{5}$$

$$SD = \sqrt{\frac{(x_1 - \bar{x})^2 + (x_2 - \bar{x})^2 + \dots + (x_n - \bar{x})^2}{n_s - 1}} \tag{6}$$

$$u_{i,typeA} = \frac{SD}{\sqrt{n_s}} \tag{7}$$

Where n is the number of times measured in the experiment. Type B is the uncertainty due to system errors which can be calculated from the following equation.

$$u_{i,typeB} = \frac{a}{\sqrt{3}} \tag{8}$$

Where a is the semi-range (or half-width) between the upper and lower limits. Combined standard uncertainty, the sum of uncertainty types A and B can be calculated from the following equation.

$$u_c = \sqrt{(u_{i,typeA})^2 + (u_{i,typeB})^2 + ...etc.} \tag{9}$$

Expanded uncertainty can be calculated from the following equation.

$$U = ku_c \tag{10}$$

Where k = 2 is correct if the combined standard uncertainty in normally distributed which gave the level of confidence of approximately 95% [41,44].

For other coverage factors (a normal distribution);
k = 1 for a confidence level of approximately 68%,
k = 2.5 for a confidence level of 99%,
k = 3 for a confidence level of 99.7%.
The results of uncertainty analysis of this study are shown in Table 3.

3. Results and discussion

According to the experiment regarding the effects of the evaporator temperature, the inclination angel and the inner diameter of TPCT on the flow patterns and heat transfer rate, the results revealed that;

3.1. Behavior of flow patterns within two - phase closed thermosyphon (TPCT)

The behavior of flow patterns within the TPCT began from the heat that evaporated through the pipe wall and the temperature of the pipe surface will gradually rise to be higher than the saturation temperature of the working fluids. Heat transfer from the pipe wall to the working fluids resulting in a decrease in the viscosity and density of the working fluid when the temperature of the evaporator increased. The temperature difference between the pipe surface temperature and the temperature of the working fluids also increased as well. The formation of a vapor bubble, thus, began to change the phase of the working fluids from liquid phase into gaseous one within the TPCT [45,46]. Bubbles flow with the accumulation of pressurized energy causing the movement of the flow pattern that comes with the flow speed. Bubbles flow caused vapor bubbles to collide and merge together resulting in the expansion of the larger vapor bubble similar to bearing which also known as the slug flow [47,48]. Collision between bubbles changes the flow pattern from the slug flow to the churn flow. When the bubbles reached a very high speed, a gap in the middle of the pipe was formed. Gas that flew in the middle of the pipe where the working fluids were liquid film was coated on the surface of the pipe which also known as annular flow. The above mentioned flow pattern is considered a basic flow pattern found in testing with TPCT where the tube's diameter were within 7 and 25.2 mm, at the angle of 80 and 90° as shown in Fig. 4. In addition stratified flow patterns and vortex flow patterns occurring in the TPCT test within the inner diameter of 25.2 mm at the inclination angel of 80 and 90° respectively. As a result, a vortex flow pattern was found at the inclination angel of 90° and at evaporation temperature of 70 and 90 °C. As per the flow characteristics of

Table 3
Uncertainty analysis result.

Type	Quantity source of uncertainty	Value of quantity	Confidence level (%)	Converge factor (k)	Standard uncertainty (ui)	Sensitivity coefficient (ci)	Uncertainty (ui ci)	Combined uncertainty component	Expanded uncertainty (u)
A	Uncertainty of mean reading (°C)	–	95	2	0.00229	1	0.00229	0.53073	1.06146
B	Thermocouple type K (°C)	−200-1372	95	2	0.86602	0.99817	0.86443		
B	Data logger (°C)	−200-1100	95	2	0.57735	0.99846	0.57646		
B	Flow meter (kg/s)	0.167–0.3	95	2	0.02886	0.39975	0.01153		

the vapor moved near the surface areas of the inner tube on both sides, gap in the middle of the was found to be the characteristic of the working fluids that is in the liquid phase which flows back from the condenser section into the evaporator section. In terms of stratified flow, there was a clear separation from each other. There was a liquid flow at the bottom of the pipe and the vapor was flowing along the top of the pipe [46,49,50]. The behavior and flow patterns that occurred within the TPCT are shown in Fig. 4. The initiated flow pattern moved up to heat the condenser section. When the working fluids was condensed and changed from vapor to liquid, the working fluids has increased in weight and moved down toward the gravity to receive the heat that the evaporator section worked continuous in a cycle.

3.2. Effects of the evaporator temperatures and the inclination angles on flow patterns

3.2.1. Upon considering the TPCT, the inner diameter 7 mm, the experimental results as shown in Table 4 (A) indicated that at the evaporator temperature 50 °C, the inclination angle of 0, 80 and 90°, no flow pattern occurred within TPCT. At this temperature, heat transferred from the hot jacket to the evaporator section which passed through the wall pipe to the working fluids is not high enough. Thus, the bonding force between the molecules of the working fluids with the particles that were the internal components of the TPCT pipe with a high value. Therefore, the heat at the evaporator temperature of 50 °C was insufficient to destroy the bond between the molecules of the working which resulted in no flow pattern. As per Table 4(B) and 4(C), when the evaporator temperatures were increased, based on the test data at the evaporator temperature of 70 and 90 °C, the inclination angle of 0, 80 and 90°, the results showed that at inclination angle of 0°, both evaporation temperatures (70 and 90 °C), there was no flow pattern within TPCT due to limitation which could not work in every test angle. The working fluid that was condensed in the liquid phase returned to the evaporator section due to the earth's gravity [45,49]. Therefore, the evaporation section must be lower. At the inclination angle of 80 and 90°, with the evaporator temperature 70 and 90 °C, four flow patterns were found which consisted of bubble flow pattern (BF), slug flow pattern (SF), churn flow pattern (CF) and annular flow pattern (AF) respectively. Due to the increase of the evaporator temperature resulting in the working fluids phase of the liquid being boiled and vaporized, a two-phase flow pattern consisting of gas flow phase and liquid flow phase were observed [13,51]. When considering the evaporator temperature of 70 and 90 °C, the inclination angle of 80°, as shown in Table 4 (B) - 4 (C), the bubble flow pattern (BF) was at 7.87% and 6.04%, while the slug flow pattern (SF) was at 10.43% and 7.82%. On the other hand, the churn flow pattern (CF) was at 25.00% and 34.37%, and the annular flow pattern (AF) was at 32.97% and 42.52% respectively. In addition, at the evaporation temperature of 70 and 90 °C, the inclination angle of 90° the bubble flow pattern (BF) was at 7.39% and 5.14%, the churn flow patterns (CF) was at 23.40% and 37.47% and the annular flow patterns (AF) was at 31.94% and 39.39% respectively.

3.2.2. Upon considering the TPCT within the inner diameter of 25.2 mm, the obtained test results as shown in Table 5 (A), 5 (B) and 5 (C) suggested that at the inclination angle of 0° the evaporator temperatures of 50, 70 and 90 °C, the flow pattern was not found
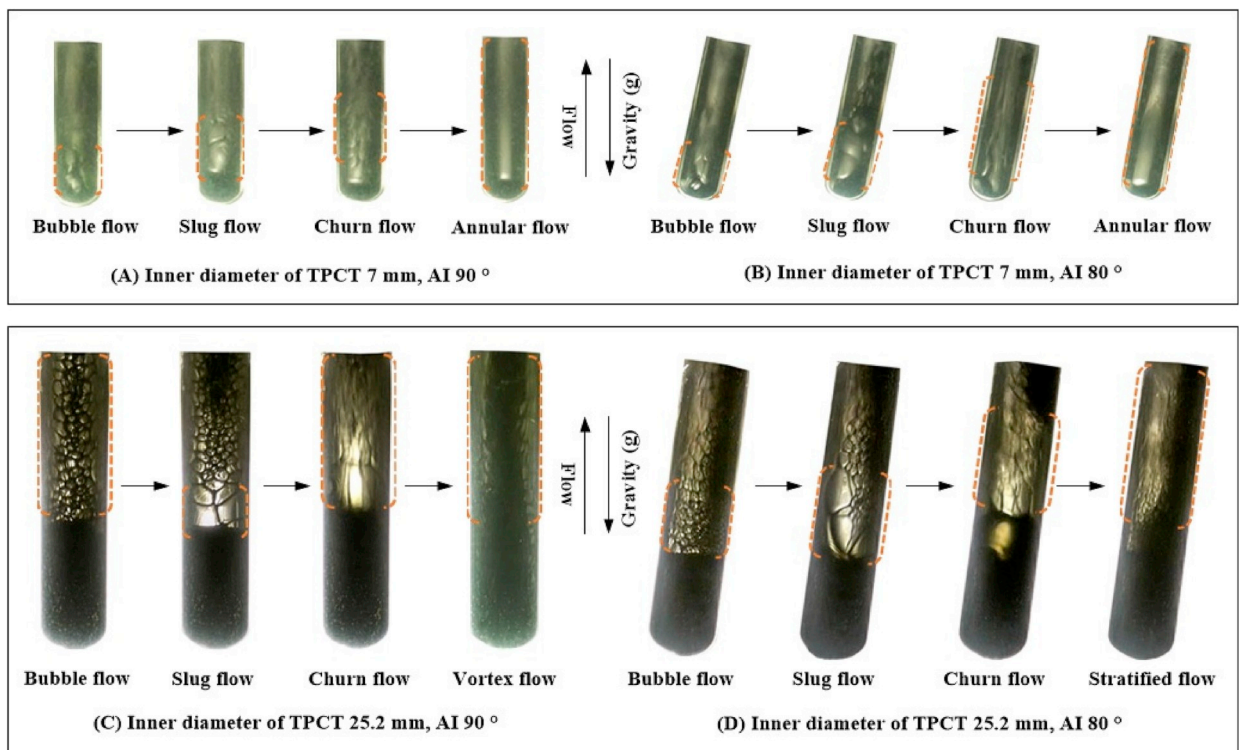

Fig. 4. Flow patterns in the TPCT with silver nanofluid with oleic acid surfactant as the working fluid.

Table 4A
Effects of the evaporator temperature and inclination angle on the flow patterns - heat transfer when using the two-phase closed thermosyphon (TPCT) within the inner diameter of 7 mm.

Tevap 50 (°C)		
The inclination angle 0°	Q (W)	q (kW/m²)
No flow patterns		
Liquid phase	1.05	1.06
The inclination angle 80° No flow patterns	Q (W)	q (kW/m²)
Liquid phase	8.54	8.63
The inclination angle 90° No flow patterns	Q (W)	q (kW/m²)
Liquid phase	8.19	8.28

within the TPCT. This was similar to the experiment results of TPCT's inner diameter 7 mm, because it was difficult to work at every angle as the working fluid would flow back to the evaporator section as a result of the earth's gravity. Therefore, the evaporation section must be lower. When considering the evaporator temperature of 50 °C at the inclination angle of 80 and 90°, as shown in Table 5 (A), the flow pattern occurred within TPCT, which was different from the experiment involved TPCT's inner diameter of 7 mm because no flow patterns were found. Due to the large diameter TPCT, the bonding force between the molecules of the working fluids with the particles was formed between the lower edge of the TPCT's inner tube. The results associated with the increasing area of heat evaporator section, and the use of working fluids containing surfactants and silver nanoparticles [52–54]. The surfactants reduces surface tension and helped to thoroughly disperse silver nanoparticles in the base fluid [13,51,55]. As a result, the base fluids achieved better boiling. At the evaporator temperature of 50 °C, the inner diameter of TPCT 25.2 mm, the inclination angle of 80°, the flow patterns were observed within the TPCT which consisted of the bubble flow pattern (BF) representing 8.67%, the slug flow pattern (SF) representing 4.94%, the churn flow pattern (CF) representing 16.90% and the stratified flow pattern (STRF-F) representing 30.72% respectively. At the inclination angle of 90°, the flow patterns found, as shown in Table 5 (A), were, the bubble flow pattern (BF) representing 38.36%, the slug flow pattern (SF) representing 9.57% and the churn flow pattern (CF) representing 34.40% respectively.

When the evaporator temperature was increased to 70 and 90 °C as shown in Table 5 (B) −5 (C), the results showed that the inclination angle of 80° resulted in the formation of stratified flow pattern (STRF-F) representing the flow pattern of 63.35% and 55.94% respectively. The vortex flow pattern (VT-F) was found at the inclination angle of 90° representing the flow pattern of 51.06% and 58.57% respectively. In the case of the vortex flow pattern, at the inclination angle of 90°, the evaporator section of the TPCT received heat from the heat source and transferred to the pipe wall of the working fluids. Working fluids were presented in the liquid phase when the heat accumulates more in the evaporator section [56,57]. As a result, the viscosity and density of the working fluids in the liquid phase were reduced simultaneously. The working fluids then began to boil and vaporize. Combining working fluids and silver nanoparticles with oleic acid helped to reduce surface tension. Addition of oleic acid also helped in dispersing nano-particle silver powder to mix with the working fluids regularly which led to the fluid-based working fluids to receive more heat in the area and led to better boiling [19,20,24,58]. Larger tube diameter resulted in a strong surface tension between the molecules of the working fluids that came into contact with the edge of the pipe wall. Therefore, when the heat was transferred from the pipe wall to the working fluids, the boiling of the working fluids a saturated liquid phase, would form vapor at the edge of the pipe wall first [45,59]. The vapor moved near the surface of the pipe on both sides because the inclination angle, in this case 90°, the TPCT was placed in a straight and

Table 4B

Effects of the evaporator temperature and inclination angle on the flow patterns - heat transfer when using the two-phase closed thermosyphon (TPCT) within the inner diameter of 7 mm.

Tevap 70 (°C)												Q (W)	q (kW/m²)
The inclination angle 0°												Q (W)	q (kW/m²)
No flow patterns													
											Liquid phase	9.41	9.51
The inclination angle 80°												Q (W)	q (kW/m²)
Annular flow (AF)			Churn flow (CF)			Slug flow (SF)			Bubble flow (BF)				
%	V_g (m/s)	L_v(m)	%	V_g (m/s)	L_v(m)	%	V_g (m/s)	L_v(m)	%	V_g (m/s)	L_v(m)		
32.97	0.4444	0.0602	25.00	0.2514	0.0126	10.43	0.0416	0.0154	7.87	0.0765	0.0057	22.12	22.37
The inclination angle 90°												Q (W)	q (kW/m²)
Annular flow (AF)			Churn flow (CF)			Slug flow (SF)			Bubble flow (BF)				
%	V_g (m/s)	L_v(m)	%	V_g (m/s)	L_v(m)	%	V_g (m/s)	L_v(m)	%	V_g (m/s)	L_v(m)		
31.94	0.3111	0.0552	23.40	0.2333	0.0391	7.39	0.0446	0.0140	1.95	0.0706	0.0079	11.32	11.45

symmetrical location. Therefore, upon observing the flow of the vapor moving on the surface of both sides of the pipe, the vapor would flow through the adiabatic section and transferred the heat to a lower temperature source and at the condenser section. When the working fluids was condensed and changed from vapor into liquid, the working fluids became heavy and moved down in the middle of the pipe and returned to the evaporator section by the gravity of the earth [60,61].

3.3. Effects of the evaporator temperature and inclination angle on the heat transfer

From Fig. 5, the relationship between the evaporator temperature and inclination angle affecting heat transfer was observed when the evaporator temperature was increased resulting in higher heat transfer values per unit area or heat flux. Due to the increase of the evaporator temperature, the evaporator section sent more heat through the pipe wall to working fluids because of differences between temperatures between the surface temperature of the pipe and the temperature of the working fluids. Therefore, the specific heat capacity of the working fluids was increased as the evaporator temperature increased. Upon combining with a higher convection coefficient from the two-phase flow pattern which consisted of gas flow phase and liquid flow phase that occurs within the TPCT, the results showed that the inclination angle of 80° with, the average heat flux was higher than that at the inclination angle 90°. At the inclination angle test position, the liquid film that was condensed in the condenser section appeared as a thin layer. As a result, the viscosity of the working fluids of the liquid phase that was ready to flow back into the evaporator section had been reduced, causing the heat resistance of the condensed liquid film to decrease as well. As for the experiment concerning TPCT with inner diameter of 7 and 25.2 mm, TPCT with inner diameter 7 mm, the inclination angle of 80°, had an average heat flux of 21.08 kW/m² which was higher than other experiments in this research. The maximum heat flux was 32.23 kW/m². At the evaporator temperature of 90 °C, which TPCT inner diameter 7 mm and the aspect ratio of 5, the length of the evaporator and the condenser section were considered relatively short. Therefore this was another reason why the vapor bubble required short and fast moving distance to go up to cool the condenser section. When considered together with the percentage of the flow pattern, as shown in Table 4 (B) - 4 (C), the results showed that the

Table 4C

Effects of the evaporator temperature and inclination angle on the flow patterns - heat transfer when using the two-phase closed thermosyphon (TPCT) within the inner diameter of 7 mm.

Tevap 90 (°C)												Q (W)	q (kW/m²)
The inclination angle 0°												Q (W)	q (kW/m²)
No flow patterns													
												13.59	13.74

Liquid phase

The inclination angle 80°												Q (W)	q (kW/m²)
Annular flow (AF)			Churn flow (CF)			Slug flow (SF)			Bubble flow (BF)				
%	V_g (m/s)	L_v(m)	%	V_g (m/s)	L_v(m)	%	V_g (m/s)	L_v(m)	%	V_g (m/s)	L_v(m)		
42.52	0.7166	0.0743	34.37	0.3619	0.0679	7.82	0.0811	0.0175	6.04	0.0939	0.0082	31.88	32.23

The inclination angle 90°												Q (W)	q (kW/m²)
Annular flow (AF)			Churn flow (CF)			Slug flow (SF)			Bubble flow (BF)				
%	V_g (m/s)	L_v(m)	%	V_g (m/s)	L_v(m)	%	V_g (m/s)	L_v(m)	%	V_g (m/s)	L_v(m)		
39.39	0.4003	0.0727	37.47	0.2083	0.0574	5.14	0.0333	0.0106	1.76	0.0833	0.0054	28.74	29.06

majority of the flow patterns were annular (AF) and churn flow patterns (CF) which were considered as the main flow patterns that affected the heat flux that obtained from the experiment involving the TPCT at the inner diameter of 7 mm, and the inclination angle of 80°. In terms of TPCT inner diameter of 25.2 mm, the results suggested that at the inclination angle of 80°, the average heat flux of 3.86 kW/m² was observed. The result was higher than the test at the inclination angle of 90° with the maximum heat flux of 5.25 kW/m² at the evaporator temperature of 90 °C. When considered in conjunction with the percentage of flow patterns as shown in Table 5 (A) - 5 (C), the majority of flow patterns were classified as stratified flow pattern (STRF-F) and churn flow patterns (CF) which were the main flow pattern that affected the heat flux as obtained from the experiment involving the TPCT with inner diameter 25.2 mm at the inclination angle of 80°.

When considering the heat flux and the evaporator temperature obtained from the TPCT, the results revealed that the evaporation of the evaporator temperature resulted in higher heat flux values due to the increased the evaporator temperature. This has caused more heat at the evaporator section to pass through the pipe wall to working fluids as a result of the temperature difference between the surface of the pipe and the working fluids. Upon combining a higher convection coefficient from the two-phase flow pattern, consisting of the gas flow phase and the liquid flow phase, that occurred within the thermosiphon [62], the characteristics of the pipe shape compared to the heat flux obtained, was found that TPCT with inner diameter of 25.2 mm, and the aspect ratio (AR) 5 had resulted in a relatively short evaporator length. The result was obtained from the calculation of the aspect ratio as shown in Fig. 5 which was compared with author's research. However, the current experimental results contrast with those of Terdtoon et al. [5], Srimuang et al. [15], and Noie et al., [63]. In regards to this study, the results were achieved using the TPCT type however with a difference in dimension and conditions. The result from Terdtoon, Srimuang and Noie demonstrated an increase of heat flux. Thus, it is important to note the vast differences among different experimental conditions, especially in regard to the type of TPCT. Due to the short evaporation length, space within the pipe and the flow distance of the working fluids was less than the internal area and the flow

Table 5A

Effects of the evaporator temperature and inclination angle on the flow patterns - heat transfer when using the two-phase closed thermosyphon (TPCT) within the inner diameter of 25.2 mm

Tevap 50 (°C)													
The inclination angle 0°												Q (W)	q (kW/m²)
No flow patterns													
												2.09	0.19

Liquid phase

The inclination angle 80°												Q (W)	q (kW/m²)
Stratified flow (Strf-F)			Churn flow (CF)			Slug flow (SF)			Bubble flow (BF)				
%	V_g (m/s)	L_v(m)	%	V_g (m/s)	L_v(m)	%	V_g (m/s)	L_v(m)	%	V_g (m/s)	L_v(m)		
30.72	0.1016	0.0573	16.90	0.0500	0.0215	4.94	0.0295	0.0130	8.67	0.0234	0.0034	32.57	2.94

The inclination angle 90°									Q (W)	q (kW/m²)
Churn flow (CF)			Slug flow (SF)			Bubble flow (BF)				
%	V_g (m/s)	L_v(m)	%	V_g (m/s)	L_v(m)	%	V_g (m/s)	L_v(m)		
34.40	0.0483	0.0387	9.57	0.0250	0.0120	38.36	0.0212	0.0038		
									29.09	2.63

distance of the working fluid at the TPCT with inner diameter 25.2 mm, caused the working fluid to transfer the heat from the evaporator section into the condenser section. This short moving distance brings the high heat flux. As for the experiment concerning TPCT with inner diameter of 7 mm, the aspect ratio (AR) 5, in comparison with the TPCT with inner diameter 25.2 mm, the results revealed that at the inclination angle of 80°, the average heat flux was 21.08 kW/m² which was higher than the heat flux obtained in other cases [8,63,64]. At the inclination angle of 80°, the liquid film in the condenser section caused the viscosity of the working fluid in the liquid phase to reduce. As a result, the heat resistance of the condensed liquid film decreases as well. In addition, the experiment using silver nanoparticles and oleic acid to reduce surface tension of the working fluid within TPCT. Whilst the working fluid is an important variable that affects the heat transfer characteristics, silver nanoparticles also help to improve the heat transfer rate due to the high thermal conductivity (k) and the presence of small particles directly affecting the contact area for receiving and exothermic heat. Furthermore, mixing of oleic acid as a surfactant helps to disperse nano-silver nanoparticles resulting in a higher proportion of heat distribution than traditional working fluid or the use of working fluid in the group of refrigerants which is useful for easy and fast boiling of working fluid.

3.4. Relationship of flow patterns-velocity and heat transfer rate

Fig. 6 shows the relationship of the flow patterns - velocity and heat transfer rate of flow patterns within the TPCT with the inner diameter of 7 mm, the aspect ratio 5, and the inclination angle of 80° and 90°. Silver powdered nanoparticles and oleic acid are used to

Table 5B

Effects of the evaporator temperature and inclination angle on the flow patterns - heat transfer when using the two-phase closed thermosyphon (TPCT) within the inner diameter of 25.2 mm

Tevap 70 (°C)								
The inclination angle 0°							Q (W)	q (kW/m²)
Not flow patterns								
							10.80	0.97
Liquid phase								
The inclination angle 80° Stratified flow (Strf-f)			Q (W)	q (kW/m²)	The inclination angle 90° Vortex flow (Vt-f)		Q (W)	q (kW/m²)
%	V_g (m/s)	L_v(m)			%	V_g (m/s) L_v(m)		
63.35	0.1600	0.0768			51.06	0.0577 0.0667		
			37.44	3.88			33.26	3.00

Table 5C

Effects of the evaporator temperature and inclination angle on the flow patterns - heat transfer when using the two-phase closed thermosyphon (TPCT) within the inner diameter of 25.2 mm

Tevap 90 (°C)								
The inclination angle 0°							Q (W)	q (kW/m²)
No flow patterns								
							14.10	1.27
Liquid phase								
The inclination angle 80° Stratified flow (Strf-f)			Q (W)	q (kW/m²)	The inclination angle 90° Vortex flow (Vt-f)		Q (W)	q (kW/m²)
%	V_g (m/s)	L_v(m)			%	V_g (m/s) L_v(m)		
55.94	0.1851	0.0700			58.57	0.0666 0.0729		
			58.15	5.25			52.06	4.70

reduce surface tension of the working fluids resulted in 4 flow patterns consisting of bubble flow pattern (BF), slug flow pattern (SF), churn flow pattern (CF) and annular flow pattern (AF) respectively. Changing of the flow pattern from one flow pattern to another is a result of the bubble flow pattern change. Such change results in alterations of flow velocity and heat transfer rate whereby the heat transfer rate has the direction and trend increasing with the flow pattern change. The flow behavior of each flow pattern varies depending on the temperature of the pipe surface which is gradually higher from the heat that evaporator section. When the surface temperature of the pipe begins to be higher than the saturation temperature of the working fluid, the heat transfer from the pipe wall to
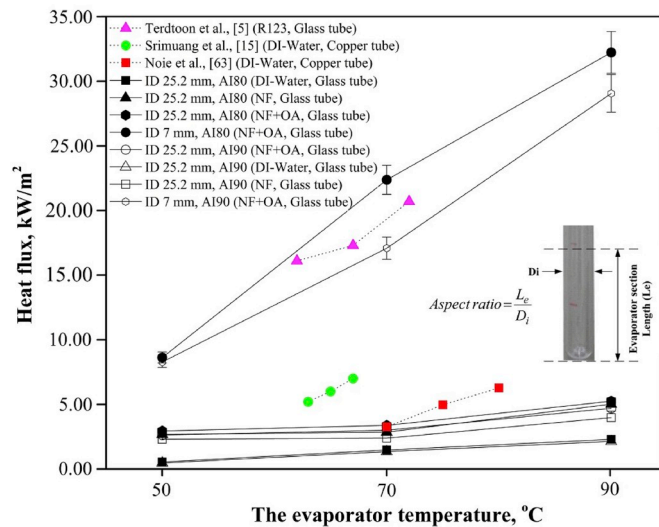
Fig. 5. Shows the relationship of the evaporator temperature and inclination angle that affected the heat flux.
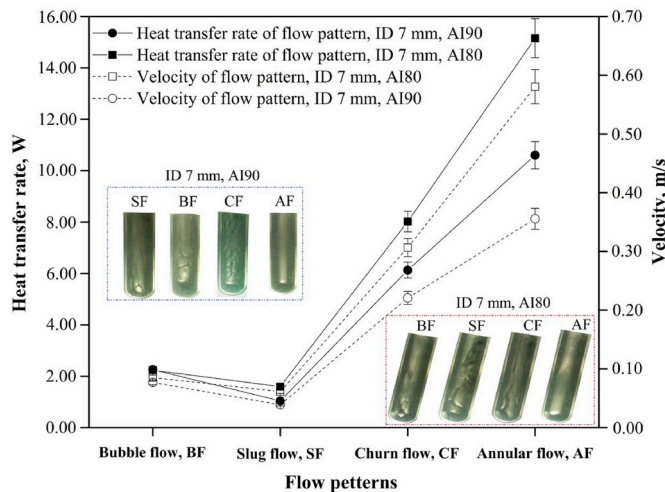

Fig. 6. Show the relationship of the flow patterns - velocity and heat transfer rate of flow patterns within the two-phase closed thermosyphon (TPCT) with the inner diameter of 7 mm and the aspect ratio 5.

the working fluid will result in the reduction of viscosity and density of working fluids in the liquid phase. The formation of a vapor bubble and the movement of the fluid are characterized by a boiling bubble with the accumulation of energy in the form of velocity and pressure. With the increasing velocity of bubble flow, the bubbles will merge until reaching the size resembling a ball bearing or the slug flow. This increases the length of the slug flow, resulting in the increase in weight of the vapor bubble and a slower velocity of the slug flow pattern. Consequently, the head of the slug flow will break due to the collision with the density and the higher velocity of the working fluid that in the gas phase which changes the churn flow pattern. The movement of the churn flow will have a high velocity resulting in a high molecular distribution of momentum which caused an increase in length of churn flow patterns. When the velocity of the bubble increases considerably, the slippery coefficient increases resulting in lower viscosity and increased flow velocity as well. This characteristic of annular flow creates a gap in the middle of the TPCT, where the gas is flowing in the middle of the TPCT. There is a liquid film working fluid on the surface of the pipe with the movement and velocity of the annular flow is higher than all flow patterns, as shown in Fig. 6.

Fig. 7 shows the relationship of the flow patterns - velocity and heat transfer rate of flow patterns within the TPCT with the inner diameter of 25.2 mm, aspect ratio 5, the inclination angle of 80° and 90°. Using silver powdered nanoparticles and oleic acid to reduce surface tension as working fluids, resulting in 4 flow patterns for the inclination angle of 80° which are; bubble flow pattern (BF), slug flow pattern (SF), churn flow pattern (CF) and stratified flow pattern (STRAF-F) respectively. At the inclination angle of 90° there were 4 flow patterns consisting of bubble flow pattern (BF), slug flow pattern (SF), churn flow pattern (CF) and vortex flow pattern (VT-F)
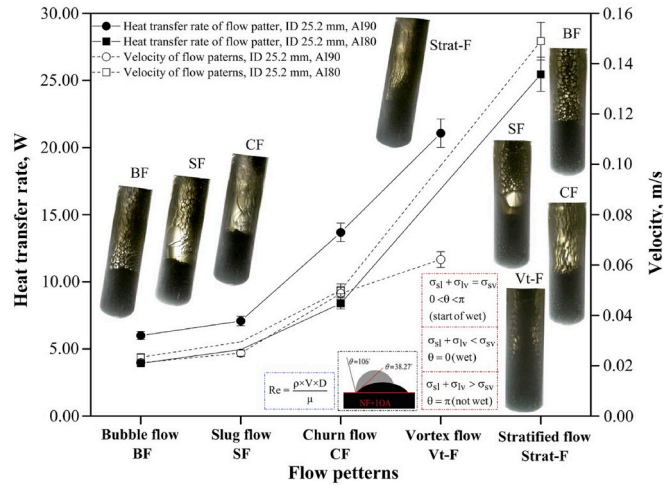
Fig. 7. Show the relationship of the flow patterns - velocity and heat transfer rate of flow patterns within the two-phase closed thermosyphon (TPCT) with the inner diameter of 25.2 mm and aspect ratio 5.

respectively. Changes of the flow pattern from one flow pattern to another resulting in changes in both flow velocity and heat transfer rate for which the heat transfer rate increased direction and trend along with the flow pattern changes from the bubble flow pattern (BF), the slug flow pattern (SF), the churn flow pattern (CF) and Separated flow pattern (STRF-F) at the inclination angle of 80°. In the case of the inclination angle of 90°, the heat transfer rate increased direction and trend along with the flow pattern change from the bubble flow pattern (BF), the slug flow pattern (SF), the churn flow pattern (CF) and the vortex flow patterns (VT-F) respectively. The flow behavior of each flow pattern varies depending on the temperature of the pipe surface which was gradually increasing. From heating to evaporator section, the surface temperature of the pipe began to be higher than the saturation temperature of the working fluid. The heat transfer from the pipe wall to the working fluids resulting in reduced viscosity and density of the working fluids in the liquid phase, causing the formation of a vapor bubble and the movement of the fluid were raised. This was characterized by a boiling bubble with the accumulation of energy in form of velocity and pressure by increasing velocity of bubble flow. The process resulted in a combination and the expansion of the bubble size which is similar to a ball bearing, also known as the slug flow. The increase in length of the slug flow led to an increase in the weight and resulting in the velocity of movement in as a slow flow. The head of the slug flow burst due to the collision with the density and the higher velocity of the working fluid of the gas phase which is considered the change to the churn flow pattern. The movement of the churn flow will have a high velocity which results in a high molecular distribution of momentum and an increased in length of churn flow patterns. When the velocity of the bubble increases considerably, the slippery coefficient also increased, resulting in lower viscosity and increased flow velocity as well. At the inclination angle of 80° the stratified flow will be observed while the inclination angle of 90°, will be observed as vortex flow. The characteristics of the stratified flow will help to reduce the flow problem or the collision between the condensed liquid flowing into the evaporator section at the bottom of the pipe and the vapor will flow along the top of the pipe, causing the flow velocity of the stratified flow to reach higher flow velocity and the heat distribution along the length of the flow. Therefore this results in the stratified and churn flow patterns as the main patterns that affects the heat transfer rate with the two- TPCT inner diameter 25.2 mm at the inclination angle of 80°. On the other hand, the heat transfer rate and velocity obtained from the stratified flow pattern and the churn flow pattern in the experiment concerning the inclination angle of 80° are 25.45, 8.39 W and 0.1489, 0.0500 m/s resulting in a more wet surface area receives heat and helps making boiling working fluids easier and better. Larger tube diameter also results in a strong surface tension between the molecules of the working fluids pulled together at the surface of the working fluids which touches the edge of the pipe. The above mentioned reason can be explained by the terms of various variables that are presented as the Reynolds number and the wet contact angle as shown in Fig. 7 [65,66] When heat is transferred from the pipe wall to the working fluids next to the pipe wall edge, the working fluids will be boiled which, in a saturated liquid phase, created vapor at the edge of the pipe wall first. The vapor are moving near the surface of the pipe on both sides because the inclination angle that is tested for the inclination angle of 90° is placed in a straight and symmetrical location. Therefore, the flow of the vapor moving on the surface of both sides of the TPCT can be observed and would float through the heat exchanger to transfer heat to a lower temperature source and condensation at the condenser section. When the working fluids are condensed and changed from vapor to liquid the fluids are weighted and move down the middle of the TPC, the fluid are then returned to the evaporator section by moving down the gravity of the earth.

4. Results

4.1 As per the experiment concerning the TPCT with inner diameter of 7 mm, the aspect ratio 5 using the working fluid of silver nanofluids with oleic acid surfactant as working fluids was observed at the inclination angle of 80 and 90°. There are four flow patterns consisting of bubble flow patterns, slug flow pattern, churn flow pattern and annular flow pattern. As for the flow behavior, the churn

and annular flow patterns exhibit high movement velocity. Therefore, this led to the heat being sent to cool at the condenser section quite quickly, and results in the long-haul movement throughout the evaporator section. Along with the convection coefficient generated by the flow patter, the flow behavior of the flow pattern directly affecting the heat transfer rate is obtained in this case study. The results indicated that churn flow pattern and annular flow pattern are the main flow patterns that affect the heat transfer rate with the inclination angle of 80 and 90°, respectively.

4.2 As per the experiment concerning the TPCT with inner diameter of 25.2 mm, the aspect ratio 5 using the working fluid of silver nanofluid with oleic acid surfactant as working fluids was studied at the inclination angle of 80 and 90°. The results suggested that bubble flow pattern, slug flow pattern, churn flow pattern, and is a basic flow pattern that can be found both in test with the inclination angle of 80 and 90°. In addition, the separated flow pattern and the vortex flow pattern also evidenced with the inclination angle of 80 and 90°, respectively. The inclination angle of 80° resulted in the stratified flow pattern which has a higher flow velocity than the churn flow pattern, slug flow patterns and bubble flow patterns. This resulted in the flow of the flow pattern that is ready to release the heat in order to cool the condenser section well and quickly. Therefore, the stratified flow pattern and churn flow pattern are the main flow pattern that affected the heat transfer rate at the inclination angle of 80°. When considering the inclination angle of 90°, the vortex flow pattern was found to have a higher flow velocity than the churn flow pattern, slug flow patterns and bubble flow pattern respectively. This is in consistence with the percentage of the occurrence of a full flow of the vortex flow patterns throughout the evaporator section. Therefore, the heat could be relieved to cool the condenser section very quickly. Therefore, the vortex flow pattern and the churn flow pattern are the main flow patterns that affected the heat transfer rate at the inclination angle of 90°.

4.3 When considering the differences in behavior and flow patterns from changing the inner diameter of the TPCT and the inclination angle, by using the working fluid of silver nanofluids with oleic acid surfactant the results suggested that, the inner diameter and the inclination angle changed have direct effect on the behavior of flow patterns. The bubble flow pattern found were, slug flow pattern and churn flow pattern as evidenced in TPCT with inner diameter of 7 and 25.2 mm and the inclination angle of 80° and 90° respectively. As for the annular flow pattern, this was only found when tested with TPCT with internal diameter 7, both the inclination angle of 80° and 90°. Stratified flow pattern was only found with TPCT inner diameter of 25.2 mm at inclination angle of 80° with a large diameter. Therefore, the separation can be clearly noticed. Furthermore, the vortex flow pattern occurs only in the case of the TPCT that was tested with the inner diameter of 25.2 mm, at inclination angle of 90°. By considering the bubble flow pattern, slug flow pattern and the churn flow pattern formed with the TPCT inner diameter of 7 mm, flow that was faster than the TPCT with inner diameter of 25.2 mm in each inclination angle of the same test was evidenced. According to the velocity of the bubble, the velocity is much higher which results in the annular flow with a short length of TPCT. This was an appropriate filling rate according to the volume of the evaporator section. Thus, easy boiling can be facilitated which causes the flow pattern that occurs with the TPCT's inner diameter of 7 mm to move at high speed for cooling at the condenser section.

4.4 The maximum heat flux obtained from the experiment was recorded at the evaporator temperature of 90 °C with the inclination angle of 80°, and the TPCT's inner diameter of 7 and 25.2 mm. The maximum heat flux obtained was 32.23 kW/m^2 when examined with TPCT's inner diameter of 7 mm at inclination angle of 80°. This was the highest heat flux in all examined samples. As for TPCT with the inner diameter of 25.2 mm, and the inclination angle of 80°, the heat flux obtained was 5.25 kW/m^2, respectively. Due to the specific heat capacity of the working fluids that was increased as the evaporator temperature increased, coupled with a higher convection coefficient from the flow pattern, and the inclination angle of 80° the liquid film condensed in the condenser section appeared as thin layer. As a result, the working fluid that flow back to the evaporator section has a lower viscosity. Higher liquidity flow also caused the heat resistance of the liquid film to decrease. In addition, the inclination angle of 80° also helps to reduce the collision or the flow between the vapor generated from the evaporator section and the liquid flowing down from the condenser section. Therefore, the inclination angle of 80° has an average heat flux throughout the test which was higher than that of the inclination angle of 90°.

Acknowledgments

Appendix A. Supplementary data

Supplementary data to this article can be found online at https://doi.org/10.1016/j.csite.2020.100586.

References

[1] D. Reay, P. Kew, Heat Pipe, Theory, Design and Application, fifth ed., Butterworth-Heinemann, 2006.

[2] T. Parametthanuwat, S. Rittidech, Heat Transfer Characteristics of the Two-phase Closed Thermosyphon (TPCT) Containing Silver Nanofluids with Oleic Acid Surfactant, Mahasarakham University, 2012.

[3] S.H. Noie, M.R. Sarmasti Emami, M. Khoshnoodi, Effect of inclination angle and filling ratio on thermal performance of a two-phase closed thermosyphon under normal operating conditions, Heat Transf. Eng. 28 (2007) 365–371, https://doi.org/10.1080/01457630601122997.

[4] A.H.A. Al-Waeli, M.T. Chaichan, K. Sopian, H.A. Kazem, Influence of the base fluid on the thermo-physical properties of PV/T nanofluids with surfactant, Case Stud. Therm. Eng. 13 (2019) 100340, https://doi.org/10.1016/J.CSITE.2018.10.001.

[5] P. Terdtoon, M. Chailungkar, M. Shiraishi, Effects of aspect ratios on internal flow patterns of an inclined closed two-phase thermosyphon at normal operating condition, Heat Transf. Eng. 19 (1998) 75–85, https://doi.org/10.1080/01457639808939938.

[6] C.K. Teoh, M.R. Maschmann, H.B. Ma, Heat-transfer analysis in heat sink embedded with a thermosyphon, J. Thermophys. Heat Transf. 17 (2003) 348–353.

[7] M. Shafai, V. Bianco, K. Vafai, O. Manca, An investigation of thermal performance of cylindrical heat pipe using nanofluids, Heat Mass Transf. 53 (2010) 376–383.

[8] P. Terdtoon, M. Chailungkar, M. Shiraishi, Effects of aspect ratios on internal flow patterns of an inclined closed two-phase thermosyphon at normal operating condition, Heat Transf. Eng. 19 (1998).

[9] K. Smith, R. Kempers, A.J. Robinson, Confinement and vapour production rate influences in closed two-phase reflux thermosyphons Part A: flow regimes, Heat Mass Transf. 119 (2018) 907–921.

[10] L.G. Asirvatham, S. Wongwises, J. Babu, Heat transfer performance of a glass thermosyphon using Graphene – acetone nanofluid, Heat Transf 137 (2015).

[11] M. Grote, M. Maximini, Z. Yang, P. Engelhardt, H. Kohne, K. Lucka, M. Brenner, Experimental and computational investigations of a compact steam reformer for fuel oil and diesel fuel, J. Power Sources 196 (2011) 9027–9035, https://doi.org/10.1016/j.jpowsour.2010.11.136.

[13] T. Paramatthanuwat, S. Boothaisong, S. Rittidech, K. Booddachan, Heat transfer characteristics of a two-phase closed thermosyphon using de ionized water mixed with silver nano, Heat Mass Transf. 46 (2010) 281–285, https://doi.org/10.1007/s00231-009-0565-y.

[14] L.J. Wei, D.Z. Yuan, Y. Feng, D.W. Tang, Experimental study of bubble growth and flow in small-diameter thermosyphon loops with filling ratios of 90% and 95%, J. Enhanc. Heat Transf. 21 (2014) 63–73.

[15] W. Srimuang, S. Rittidech, B. Bubphachot, Heat transfer characteristics of a vertical flat thermosyphon (VFT), J. Mech. Sci. Technol. 23 (2009) 2548–2554, https://doi.org/10.1007/s12206-009-0703-y.

[16] E.O. Agunlejika, P. Langston, B.J. Azzopardi, B.N. Hewakandamby, Flow instabilities in a horizontal thermosyphon reboiler loop, Exp. Therm. Fluid Sci. 78 (2016) 90–99.

[17] X. Huo, L. Chen, Y.S. Tian, T.G. Karayiannis, Flow boiling and flow regimes in small diameter tubes. Applied Thermal Engineering, Appl. Therm. Eng. 24 (2004) 1225–1239.

[18] N. Bhuwakietkumjohn, S. Rittidech, Internal flow patterns on heat transfer characteristics of a closed-loop oscillating heatpipe with check valves using ethanol and a silver nano-ethanol mixture, Exp. Therm. Fluid Sci. 34 (2010) 1000–1007.

[19] T. Parametthanuwat, S. Rittidech, Silver nanofluid containing oleic acid surfactant as working fluid in the two-phase closed thermosyphon (TPCT): a thermodynamic study, Nanoscale Microscale Thermophys. Eng. 17 (2013) 216–235, https://doi.org/10.1080/15567265.2013.776652.

[20] S.U.S. Choi, Nanofluids, A new field of scientific research and innovative applications, Heat Transf. Eng. 29 (2008) 429–431, https://doi.org/10.1080/01457630701850778.

[21] A.E. Kabeel, T.A. El Maaty, Y. El Samadony, The effect of using nano-particles on corrugated plate heat exchanger performance, Appl. Therm. Eng. 52 (2013) 221–229, https://doi.org/10.1016/j.applthermaleng.2012.11.027.

[22] S. Khandekar, Y.M. Joshi, B. Mehta, Thermal performance of closed twop-hase thermosyphon using nanofluids, Int. J. Therm. Sci. 47 (2008) 659–667.

[23] E. Firouzfar, M. Soltanieh, S.H. Noie, M.H. Saidi, Investigation of heat pipe heat exchanger effectiveness and energy saving in air conditioning systems using silver nanofluid, Int. J. Environ. Sci. Technol. 9 (2012) 587–594, https://doi.org/10.1007/s13762-012-0051-9.

[24] S.H. Noie, S.Z. Heris, M. Kahani, S.M. Nowee, Heat transfer enhancement using Al2O3/water nanofluid in a two-phase closed thermosyphon, Int. J. Heat Fluid Flow 30 (2009) 700–705, https://doi.org/10.1016/j.ijheatfluidflow.2009.03.001.

[25] M. Ghanbarpour, N. Nikkam, R. Khodabandeh, M.S. Toprak, Improvement of heat transfer characteristics of cylindrical heat pipe by using SiC nanofluids, Appl. Therm. Eng. 90 (2015) 127–135.

[26] R. S, S. I, T. M, KUMAR, AN experimental investigation OF the thermal performance OF two-phase closed thermosyphon using zirconia nanofluid, Therm. Sci. 20 (2016) 1565–1574.

[27] M.H. Buschmann, U. Franzke, Improvement of thermosyphon performance by employing nanofluid, Int. J. Refrig. 40 (2014) 416–428.

[28] X.-F. Yang, Z.-H. Liu, Flow boiling heat transfer in the evaporator of a loop thermosyphon operating with CuO based aqueous nanofluid, Heat Mass Transf. 55 (2012) 7375–7384.

[29] K.H. Do, H.J. Ha, S.P. Jang, Thermal resistance of screen mesh wick heat pipes using the water-based Al2O3 nanofluids, Heat Mass Transf. 53 (2010) 5888–5894.

[30] Z.H. Liu, Q.Z. Zhu, Application of aqueous nanofluids in a horizontal mesh heat pipe, Energy Convers. Manag. 52 (2011) 292–300, https://doi.org/10.1016/j.enconman.2010.07.001.

[31] D. Wasan, A. Nikolov, B. Moudgil, Colloidal dispersions: structure, stability and geometric confinement, Powder Technol. 153 (2005) 135–141.

[32] D.W.Y. Ding, Particle migration in a flow of nanoparticle suspensions, Powder Technol. 149 (2005) 84–92.

[33] Y. Hwang, J.K. Lee, Y.M. Jeong, S.I. Cheong, Y.C. Ahn, S.H. Kim, Production and dispersion stability of nanoparticles in nanofluids, Powder Technol. 186 (2008) 145–153, https://doi.org/10.1016/j.powtec.2007.11.020.

[34] T.P. Teng, Y.H. Hung, T.C. Teng, H.E. Mo, H.G. Hsu, The effect of alumina/water nanofluid particle size on thermal conductivity, Appl. Therm. Eng. 30 (2010) 2213.

[35] R. Savino, R. Di Paola, D.M. Gattia, R. Marazzi, M.V. Antisari, Self-rewetting fluids with suspended carbon nanostructures, J. Nanosci. Nanotechnol. 11 (2011) 8953–8958, https://doi.org/10.1166/jnn.2011.3495.

[36] X.F. Li, D.S. Zhu, X.J. Wang, N. Wang, J.W. Gao, H. Li, Thermal conductivity enhancement dependent pH and chemical surfactant for Cu-H2O nanofluids, Thermochim. Acta 469 (2008) 98–103.

[37] K. S, B. M, M.A. Khairul Elham Doroodchi, Reza Azizian, Effects of surfactant on stability and thermo-physical properties of metal oxide nanofluids, Heat Mass Transf. 98 (2016) 778–787.

[38] L. Vékás, D. Bica, O. Marinica, Magnetic nanofluids stabilized with various chain length surfactants, Rom. Rep. Phys. 58 (2006) 257–267.

[39] K. Lu, C. Kessler, Colloidal dispersion and rheology study of nanoparticles, J. Mater. Sci. 41 (2006) 5613–5618.

[40] T. Parametthanuwat, N. Bhuwakietkumjohn, S. Rittidech, Y. Ding, Experimental investigation on thermal properties of silver nanofluids, Heat Fluid Flow 56 (2015) 80–90.

[41] S. Bell, A beginner's guide to uncertainty of measurement. Beginner's Guid. To Uncertainty Meas., National Physical Laboratory, Middlesex, 2001.

[42] Frank P. Incropera, D.P. Dewitt, Fundamental of Heat and Mass Transfer, fourth ed., John Wiley & Son, New York, 1996 fourth ed.

[44] N. Pipatpaiboon, S. Rittidech, P. Meena, Experimental study of a thermosyphon heat exchanger (TPHE) in a bio-diesel factory in Thailand, Arabian J. Sci. Eng. 37 (2012) 2047–2060, https://doi.org/10.1007/s13369-012-0310-6.

[45] G.S.H. Lock, The Tubular Thermosyphon Variations on a Theme, Oxford University Press, New York: United State, 1992.

[46] S. Tamaki, Y. Fujii, Y. Matsushita, H. Aoki, T. Miura, K. Take, H. Hamano, Effects of an internal heat exchanger in a refrigerant system with carbon dioxide on its cooling coefficient of performance and cooling capacity, Kagaku Kogaku Ronbunshu 34 (2008) 505–512, https://doi.org/10.1252/kakoronbunshu.34.505.

[47] T. Payakaruk, P. Terdtoon, S. Ritthidech, Correlations to predict heat transfer characteristics of an inclined closed two-phase thermosyphon at normal operating conditions, Appl. Therm. Eng. 20 (2000) 781–790. http://www.sciencedirect.com/science/article/pii/S1359431199000472. (Accessed 14 September 2011).

[48] S. Liu, J.T. Li, Q. Chen, Visualization of flow pattern in thermosyphon by ECT, Flow Meas, Instrumentation 18 (2007) 216–222, https://doi.org/10.1016/j.flowmeasinst.2007.06.012.

[49] P. Terdtoon, Boiling, Chiang Mai University, 2001.

[50] N. Lamaison, J.B. Marcinichen, S. Szczukiewicz, J.R. Thome, P. Beucher, Passive two-phase thermosyphon loop cooling system for high-heat-flux servers, Interfacial Phenom. Heat Transf. 3 (2015) 369–391, https://doi.org/10.1615/InterfacPhenomHeatTransfer.2016015637.

[51] S. Khandekar, Y.M. Joshi, B. Mehta, Thermal performance of closed two-phase thermosyphon using nanofluids, Int. J. Therm. Sci. 47 (2008) 659–667, https://doi.org/10.1016/j.ijthermalsci.2007.06.005.

[52] T. Inoue, M. Monde, Operating limit of heat transport in two-phase thermosyphon with connecting pipe (heated surface temperature fluctuation and flow pattern), Int. J. Heat Mass Transf. 52 (2009) 4519–4524, https://doi.org/10.1016/j.ijheatmasstransfer.2009.03.062.

[53] T. Parametthanuwat, S. Rittidech, A. Pattiya, Y. Ding, S. Witharana, Application of silver nanofluid containing oleic acid surfactant in a thermosyphon economizer, Nanoscale Res. Lett. 6 (2011) 315, https://doi.org/10.1186/1556-276X-6-315.

[54] C.Y. Park, P.S. Hrnjak, CO2 and R410A flow boiling heat transfer, pressure drop, and flow pattern at low temperatures in a horizontal smooth tube, Int. J. Refrig. Int. Du Froid. 30 (2007) 166–178, https://doi.org/10.1016/j.ijrefrig.2006.08.007.

[55] N. Bhuwakietkumjohn, T. Parametthanuwat, Heat transfer behaviour of silver particles containing oleic acid surfactant: application in a two phase closed rectangular cross sectional thermosyphon (RTPTC), Heat Mass Transf. 53 (2017) 37–48, https://doi.org/10.1007/s00231-016-1798-1.

[56] J. Cousin, H.J. Nuglisch, Modeling of internal flow in high pressure swirl injectors, SAE Tech. Pap. Ser. (2010), https://doi.org/10.4271/2001-01-0963.

[57] S. Lewis, W.L. Fu, G. Kojasoy, Internal flow structure description of slug flow-pattern in a horizontal pipe, Int. J. Heat Mass Transf. (2002), https://doi.org/10.1016/S0017-9310(02)00107-2.

[58] T. Parametthanuwat, N. Bhuwakietkumjohn, Application of nanofluid in thermosyphon (TPCT) - a review, in: J.N. Govil (Ed.), Nanotechnol. Fundam. Appl., Studium Press LLC., U.S.A, 2013, pp. 293–310.

[59] I. Khazaee, R. Hosseini, S.H. Noie, Experimental investigation of effective parameters and correlation of geyser boiling in a two-phase closed thermosyphon, Appl. Therm. Eng. 30 (2010) 406–412, https://doi.org/10.1016/j.applthermaleng.2009.09.012.

[60] A. Franco, S. Filippeschi, Closed loop two-phase thermosyphon of small dimensions: a review of the experimental results, Microgravity Sci. Technol. 24 (2012) 165–179, https://doi.org/10.1007/s12217-011-9281-6.

[61] K. Smith, S. Siedel, A.J. Robinson, R. Kempers, The effects of bend angle and fill ratio on the performance of a naturally aspirated thermosyphon, Appl. Therm. Eng. (2016), https://doi.org/10.1016/j.applthermaleng.2016.01.024.

[62] J.T. Cieslinski, A. Fiuk, Heat transfer characteristics of a two-phase thermosyphon heat exchanger, Appl. Therm. Eng. 51 (2013) 112–118, https://doi.org/10.1016/j.applthermaleng.2012.08.067.

[63] S.H. Noie-Baghban, Heat transfer characteristics of a two phase closed thermosyphon, Appl. Therm. Eng. 25 (2005) 495–506.

[64] P. Amtachaya, W. Srimuang, Comparative heat transfer characteristics of a flat two-phase closed thermosyphon (FTPCT) and a conventional two-phase closed thermosyphon (CTPCT), Heat Mass Transf. 37 (2010) 293–298.

[65] A. Nurpeiis, A. Nee, Mathematical modelling OF force convection IN a two–phase thermosyphon IN conjugate formulation, EPJ Web Conf. 110 (2016) 1–7.

[66] A. Amiri, M. Shanbedi, H. Eshghi, S.Z. Heris, M. Baniadam, Highly dispersed multiwalled carbon nanotubes decorated with Ag nanoparticles in water and experimental investigation of the thermophysical properties, J. Phys. Chem. C 116 (2012) 3369–3375, https://doi.org/10.1021/Jp210484a.